Journal of Achievements in Materials and Manufacturing Engineering
VOLUME 38
ISSUE 1
January
2010

Dry friction of bearings on dynamics and control of an inverted pendulum

D. Guida*, F. Nilvetti, C.M. Pappalardo
Mechanical Engineering Department, University of Salerno,
Via Ponte Don Melillo, Fisciano, SA, 84084, Italy
* Corresponding author: E-mail address: guida@unisa.it

Received 22.11.2009; published in revised form 01.01.2010

Analysis and modelling

ABSTRACT

Purpose: Investigation of dry friction parameters on the control system of a cart pendulum.
Design/methodology/approach: A geometrical approach has been used to analyze the influence of bearing friction on the cart-pendulum dynamics. This approach was developed by one of authors in the paper " Influence of the Variation between Static and Kinetic Friction on Stick-Slip Instability" pubblished by WEAR 1993.
Findings: Relations that allow us to evaluate how the friction parameters of bearings influence the performances of the control system of a cart-pendulum.
Research limitations/implications: The "a priori knowing" of friction parameters is the intrinsic limitation of this method.
Originality/value: A novel methodology for designing of more effective control systems.
Keywords: Engineering design; Applied mechanics; Dry friction; Inverted pendulum; Optimal control

Reference to this paper should be given in the following way:
D. Guida, F. Nilvetti, C.M. Pappalardo, Dry friction of bearings on dynamics and control of an inverted pendulum, Journal of Achievements in Materials and Manufacturing Engineering 38/1 (2010) 80-94.

1. Introduction

Stabilization of the inverted pendulum on a cart is one of the most interesting problems in nonlinear control theory. This mechanical device consists of a free vertical rotating pendulum with a pivot point mounted on a cart, the cart can move itself horizontally. The control action is a horizontal force on the cart. Due to the fact that the angular acceleration of the vertical pendulum cannot be directly controlled, the inverted pendulum is an interesting example of an under-actuated mechanical system. For this system in frictionless condition a lot of control laws have been introduced. Some other control laws have been suggested considering a friction without discontinuity in zero velocity.
There are two important problems related to the stabilization of this device. The first is swinging the pendulum up from the hanging position to the upright vertical position. The second problem consists in stabilization of the inverted pendulum around its unstable equilibrium point. In this paper is analyzed the dry friction influence on the stability of the inverted pendulum control system.

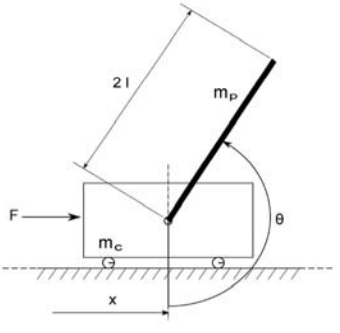

Fig. 1. Cart Pendulum

2. Mathematical model of a cart pendulum

The equations of motion of the cart and pendulum in Figure 1 is:

$$\begin{aligned}(m_p + m_s)\ddot{x} + lm_p \sin(\theta)\ddot{\theta} - lm_p \sin(\theta)\dot{\theta}^2 &= F + F_{fric} \\ \frac{4}{3}l^2 m_p \ddot{\theta} + glm_p \sin(\theta) + lm_p \cos(\theta)\ddot{x} &= C_{fric}\end{aligned} \quad (1)$$

where x is the position of the cart, θ is the pendulum angle, measured in degrees away from stable equilibrium position, F is the force applied to the cart and, F_{fric} and C_{fric} are, respectively, the friction force between cart and linear guide and the friction torque in the pivot point of the pendulum. A feedback controller was designed for this system, to balance the pendulum in the upright position. The controller was designed using an optimal linear quadratic controller. Equations (1) were used to model the open-loop inverted pendulum during simulations. However, for the design of the linear state-feedback controller, used for stabilization, a linearized version of these equations was used. The inverted position of the pendulum corresponds to the unstable equilibrium point $(x, \theta, \dot{x}, \dot{\theta}) = (0, \pi, 0, 0)$.

This corresponds to the origin of the state space. Using these approximations in Equations (1), the mathematical model linearized around the unstable equilibrium point of the inverted pendulum is obtained, and it is given by the following equations:

$$\begin{aligned}\ddot{x} &= \frac{1}{m_c + m_p}(F - lm_p\ddot{\tilde{\theta}}) \\ \ddot{\tilde{\theta}} &= \frac{3}{4l^2 m_p}(glm_p\tilde{\theta} - lm_p\ddot{x})\end{aligned} \quad (2)$$

where $\tilde{\theta} = \pi - \theta$ is a change of reference.

To get these two equations into valid state space matrix form both $\ddot{x}$ and $\ddot{\theta}$ must be functions of lower order terms only. Writing the resulting equations in matrix form, the linearized state-space model is obtained and is given by the matrix linear Equations (3) and (4).

$$\dot{z} = \begin{bmatrix} 0 & 0 & 1 & 0 \\ 0 & 0 & 0 & 1 \\ 0 & -\dfrac{3gm_p}{m_p + 4m_c} & 0 & 0 \\ 0 & \dfrac{3g(m_p + m_c)}{l(m_p + 4m_c)} & 0 & 0 \end{bmatrix} z + \begin{bmatrix} 0 \\ 0 \\ \dfrac{4}{m_p + 4m_c} \\ -\dfrac{3}{l(m_p + 4m_c)} \end{bmatrix} F \quad (3)$$

$$y = \begin{bmatrix} 1 & 0 & 0 & 0 \\ 0 & 1 & 0 & 0 \\ 0 & 0 & 1 & 0 \\ 0 & 0 & 0 & 1 \end{bmatrix} z \quad (4)$$

Where z is the state vector ($\begin{bmatrix} x & \tilde{\theta} & \dot{x} & \dot{\tilde{\theta}} \end{bmatrix}^T$) and y is the output vector (y=z).

3. LQ optimal regulation

In optimal control one attempt to find a controller that provides the best possible performance with respect to some given index of performance. E.g., the controller that uses the least amount of control-signal energy to take the output to zero. In this case the index of performance would be the control signal energy. When the mathematical model of the system to be controlled is linear and the functions that appear in the index of performance are quadratic forms, we have a problem of LQ optimal control. More generally, the state-space model of the process is in the form:

$$\dot{z}(t) = A(t)z(t) + B(t)u(t), \quad (5)$$

$$y(t) = C(t)z(t) \quad (6)$$

The index of performance is given by:

$$J_{LQ} := z^T(t_f)S_f(t_f) + \int_{t_0}^{t_f} [y^T(t)Q(t)y(t) + u^T(t)R(t)u(t)]dt \quad (7)$$

with $S_f = S_f^T \geq 0$, $Q(t) = Q^T(t) > 0$, $R(t) = R^T(t) > 0$, $\forall t \in [t_0, t_f]$ and t_f assigned. Generally the components of the vector y(t) does not coincide with the *measured output*, but generally, they are special linear combinations of state variables that you want to keep close to zero (*controlled output*).

It required that the S_f, $Q(t)$ and $R(t)$ matrices are positive semidefinite, because, generally, you want to penalize vectors z(t) and u(t) deviations from their respective origins of vector spaces. The elements on the diagonal of the matrix S_f, $Q(t)$ and $R(t)$ have an immediate interpretation, because they penalize the squares of the individual components of the vectors $z(t)$, $y(t)$ and $u(t)$: therefore, the matrices S_f, $Q(t)$ and $R(t)$ are usually chosen diagonals.

The term

$$\int_{t_0}^{t_f} u^T(t)R(t)u(t)\,dt \quad (8)$$

corresponds to the *energy of the controlled output* and the term

$$\int_{t_0}^{t_f} y^T(t)Q(t)y(t)\,dt \quad (9)$$

corresponds to the *energy of the control signal*.

It can be shown that the solution of the LQ problem can be realized as algebraic linear feedback of state variables:

$$u(t) = -K(t)z(t) \quad (10)$$

with, $K(t) = R^{-1}(t)B^T(t)S(t)$, where the matrix $S(t)$ is solution of the differential Riccati equation.

Considering the linear model stationary, stabilizable and detectable:

$$\begin{aligned}\dot{z}(t) &= Az(t) + Bu(t), \\ y(t) &= Cz(t)\end{aligned} \quad (11)$$

The problem of regulation (LQ) in infinite time is to determine the optimal feedback control law which minimizes the performance index:

$$J_{LQ} := \int_{t_0}^{\infty} [y^T(t)Qy(t) + u^T(t)Ru(t)]dt \tag{12}$$

where $Q = Q^T > 0$ and $R = R^T$. The solution is given by the control law:

$$u(t) = -Kz(t), \qquad K := R^{-1}B^T S \tag{13}$$

where the symmetric matrix S is the unique positive semidefinite solution of the *algebric Riccati equation* (ARE).

A more general formulation, the index of performance, is as follows:

$$J_{LQ} := \int_{t_0}^{\infty} \left[y^T(t)Qy(t) + 2y^T(t)Nu(t) + u^T(t)Ru(t) \right] dt = \\ = \int_{t_0}^{\infty} \left[y^T(t) \quad u^T(t) \right] \begin{bmatrix} Q & N \\ N^T & R \end{bmatrix} \begin{bmatrix} y(t) \\ u(t) \end{bmatrix} dt \tag{14}$$

with $N > 0$.

This formulation is useful, for example, to solve problems of regulation that preview a term which penalizes the derivatives of state variables.

In this case:

$$K = R^{-1}\left(B^T S + N^T C\right) z(t) \tag{15}$$

and S is the unique positive semidefinite solution of the ARE.

The stabilizing control law is designed applying the LQ methods to the model without friction linearized at the upward equilibrium point:

$$(x, \theta, \dot{x}, \dot{\theta}) = (0, \pi, 0, 0) \tag{16}$$

The final control law from this design, is the result of a matrix multiplication between the state vector $\underline{z}$ and a gain matrix of compatible dimensions K, such that $F = -K\underline{z}$.

Where K is designed as the matrix that minimizes the following cost function:

$$J_{LQ} := \int_0^{\infty} \left[\underline{z}^T Q \underline{z} + \rho F^2 \right] dt \tag{17}$$

Where Q is an 4×4 symmetric positive-definite matrix and ρ a positive constant.

The matrix Q and the constant ρ are chosen by applying the following rule:

$$Q_{ii} = \frac{1}{\text{maximum acceptable value of } z_i^2}, \quad i \in \{1, 2, \ldots, 4\} \tag{18}$$

$$\rho = \frac{1}{\text{maximum acceptable value of } F^2} \tag{19}$$

Q and ρ are choosing in order to penalize more the non-zero position.

Considering for the system in figure 1:

$$\begin{aligned} m_c &= 0.6953\text{kg}, \\ m_p &= 0.0667\text{kg}, \\ l &= 0.1430\text{m} \end{aligned} \tag{20}$$

This reasoning led to

$$Q = diag(6.2500,\ 6.2500,\ 0.0016,\ 0.0001) \tag{21}$$

and

$$\rho = 0.2500 \tag{22}$$

With Q and ρ as above is obtained the feedback gain:

$$K = [k1,\ k2,\ k3,\ k4] = \\ = [-5.0000,\ -25.2465,\ -4.2579,\ -3.3797] \tag{23}$$

In figure 2 and 3 is showed the response of the system following a small perturbation of the equilibrium point in the initial conditions:

$$(x_0, \theta_0, \dot{x}_0, \dot{\theta}_0) = (0, \pi + \Delta, 0, 0) \tag{24}$$

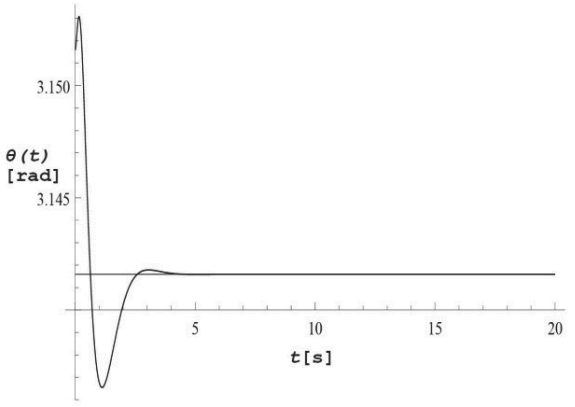

Fig. 2. Pendulum displacement vs. time in frictionless condition

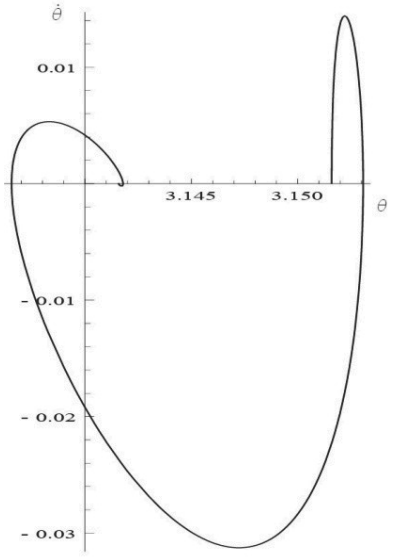

Fig. 3. Angular velocity vs. angular rotation of pendulum in frictionless condition

4. Friction models overview

In this section a brief summary of friction models [1] is given.

4.1. Static models

Classic models

The classical models of friction consist of different components, which each take care of certain aspects of the friction force.

Coulomb friction

The main idea is that friction opposes motion and that its magnitude is independent of velocity and contact area. It can therefore be described as

$$F = F_C \text{sgn}(v) \tag{25}$$

where the friction force F_C is proportional to the normal load:

$$F_C = \mu N \tag{26}$$

This description of friction is termed *Coulomb friction*. This model is an ideal relay model. The Coulomb friction model does not specify the friction force for zero velocity. It may be zero or it can take on any value in the interval between $-F_C$ and F_C, depending on how the sign function is defined. The Coulomb friction model has, because of its simplicity, often been used whit friction model.

Viscous friction

In the 19th century the theory of hydrodynamics was developed leading to expressions for the friction force caused by the viscosity of lubricants. The term *viscous friction* is used for this force component, which is normally described as:

$$F = F_v v \tag{27}$$

Coulomb and viscous friction

Viscous friction is often combined with Coulomb friction:

$$F = F_v |v| \text{sgn}(v) \tag{28}$$

Better fit to experimental data can often be obtained by a nonlinear dependence on velocity:

$$F = F_v |v|^{\delta_v} \text{sgn}(v) \tag{29}$$

where δ_v depends on the geometry of the application.

Static friction

Static friction describes the friction force at rest. [2] introduced the idea of a friction force at rest that is higher than the Coulomb friction level. Static friction counteracts external forces below a certain level and thus keeps an object at rest.

It is hence clear that friction at rest cannot be described as a function of only velocity. Instead it has to be modeled using the external force F_e in the following manner:

$$F = \begin{cases} -F_e & \text{if } v = 0 \text{and} |F_e| < F_S \\ -F_S \text{sgn}(F_e) & \text{if } v = 0 \text{and} |F_e| \geq F_S \end{cases} \tag{30}$$

The friction force for zero velocity is a function of the external force and not the velocity. The traditional way of depicting friction in block diagrams with velocity as the input and force as the output is therefore not completely correct. If doing so, stiction must be expressed as a multi-valued function that can take on any value between the two extremes $-F_S$ and F_S. Specifying stiction in this way leads to non-uniqueness of the solutions to the equations of motion for the system.

The classical friction components can be combined in different ways and any such combination is referred to as a classical model. These models have components that are either linear in velocity or constant. Stribeck observed in [3] that the friction force does not decrease discontinuously but that the velocity dependence is continuous. This is called Stribeck friction. A more general description of friction than the classical models is, therefore:

$$F = \begin{cases} F(v) & \text{if } v \neq 0 \\ -F_e & \text{if } v = 0 \text{and} |F_e| < F_S \\ -F_S \text{sgn}(F_e) & \text{if } v = 0 \text{and} |F_e| \geq F_S \end{cases} \tag{31}$$

where $F(v)$ is an arbitrary function of velocity. A number of parameterizations of $F(v)$ have been proposed, see [4]. A common form of the nonlinearity is:

$$F(v) = F_C + (F_S - F_C) e^{-|v/v_S|^{\delta_S}} + F_v v \tag{32}$$

where v_S is called the Stribeck velocity. Such models have been used for a long time. The function F is easily obtained by measuring the friction force for motions with constant velocity. The curve is often asymmetrical.

The Karnopp Model

The model presented by karnopp in [5], attempts to overcome the problems that exist in previous models to identify when the speed is zero and to avoid switching between different state equation for sticking and sliding. The model defines a zero velocity interval, $|v| < \Delta V$. For velocities within this interval the internal state of the system (the velocity) may change and be non-zero but the output of the block is maintained at zero by a dead-zone. Depending on if $|v| < \Delta V$ or not, the friction force is either a saturated version of the external force or an arbitrary static function of velocity.

The drawbacks with the model are that the external force is an input to the model and this force is not always explicitly given, besides the zero velocity interval does not agree with real friction.

Armstrong's Model

This model, proposed by Armstrong in [4] introduces temporal dependencies for static friction and Stribeck effect, but does not handle pre-sliding displacement. This is instead done by describing the sticking behavior by a separate equation. Some mechanism must then govern the switching between the model for sticking and the model for sliding. The friction is described by

$$F(x) = \sigma_0 x \tag{33}$$

when sticking and by

$$F(v,t) = F_v v + \left(F_C + F_S(\gamma, t_d) \frac{1}{1 + \left(v(t - \tau_l) / v_S \right)^2} \right) \text{sgn}(v) \tag{34}$$

when sliding,where

$$F_S(\gamma, t_d) = F_{S,a} + \left(F_{S,\infty} - F_{S,a} \frac{t_d}{t_d + \gamma} \right) \tag{35}$$

$F_{S,a}$ is the Stribeck friction at the end of the previous sliding period and t_d the dwell time, i.e., the time since becoming stuck.

The model requires a parameter to determine the switching between two separate models that compose it. Furthermore, the model states have to be initialized appropriately every time a switch occurs.

4.2. Dynamic models

The Dahl Model

The starting point for Dahl's model is the stress-strain curve in classical solid mechanics, see [6] and [1]. When subject to stress the friction force increases gradually until rupture occurs. Dahl modeled the stress-strain curve by a differential equation. Let x be the displacement, F the friction force, and F_c the Coulomb friction force. Then Dahl's model has the form:

$$\frac{dF}{dx} = \sigma \left(1 - \frac{F}{F_c} \operatorname{sgn}(v) \right)^{\alpha} \tag{36}$$

where σ is the stiffness coefficient and α is a parameter that determines the shape of the stress-strain curve. The valuea $\alpha = 1$ is most commonly used.

The friction force $|F|$ will never be larger than F_c if its initial value is such that $|F(0)| < F_c$.

Notice that in this model the friction force is only a function of the displacement and the sign of the velocity. This implies that the friction force is only position dependent.
To obtain a time domain model Dahl observed that:

$$\frac{dF}{dt} = \frac{dF}{dx}\frac{dx}{dt} = \frac{dF}{dx} v = \sigma \left(1 - \frac{F}{F_c} \operatorname{sgn}(v) \right)^{\alpha} v \tag{37}$$

The model is a generalization of ordinary Coulomb friction. The Dahl model neither captures the Stribeck effect, which is a rate dependent phenomenon, nor does it capture static friction.

The Bristle Model

Haessig and Friedland introduced a friction model in [7], which attempted to capture the behavior of the microscopical contact points between two surfaces. Each point of contact is thought of as a bond between flexible bristles. As the surfaces move relative to each other the strain in the bond increases and the bristles act as springs giving rise to a friction force. The force is then given by:

$$F = \sum_{i=1}^{N} \sigma_0 \left(x_i - b_i \right) \tag{38}$$

where N is the number of bristles, σ_0 the stiffness of the bristles, x_i the relative position of the bristles, and b_i the location where the bond was formed. As $|x_i - b_i|$ equals δ_s the bond snaps and a new one is formed at a random location relative to the previous location.

Reset Integrator Model

This model, always introduced in [7], can be viewed as an attempt to make the bristle model computationally feasible. Instead of snapping a bristle the bond is kept constant by shutting off the increase of the strain at the point of rupture. The model utilizes an extra state to determine the strain in the bond, which is modeled by:

$$\frac{dz}{dt} = \begin{cases} \text{if } \left(v > 0 \text{and} z \geq z_0 \right) \\ 0 \qquad \text{or} \\ \left(v < 0 \text{and} z \leq -z_0 \right) \\ v \quad \text{otherwise} \end{cases} \tag{39}$$

The friction force is given by:

$$F = \left(1 + a(z) \right) \sigma_0 (v) z + \sigma_1 \frac{dz}{dt} \tag{40}$$

where $\sigma_1 dz/dt$ is a damping term that is active only when sticking, while, the static friction is achieved by the function $a(z)$, which is given by:

$$a(z) = \begin{cases} a \quad \text{if } |z| < z_0 \\ 0 \quad \text{otherwise} \end{cases} \tag{41}$$

The Bliman and Sorine Model

Bliman and Sorine have developed a family of dynamic models in a series of papers [8]. The magnitude of the friction depends only on sgn (v) and the space variable s defined by:

$$s = \int_0^t |v(\tau)| d\tau \tag{42}$$

The models are expressed as linear systems in the space variable s:

$$\begin{aligned} \frac{dx_s}{ds} &= Ax_s + Bv_s \\ F &= Cx_s \end{aligned} \tag{43}$$

The variable $v_s = \operatorname{sgn}(v)$ is required to obtain the correct sign. Bliman and Sorine have models of different complexity. The first order model is given by:

$$A = -1/\varepsilon_f, \quad B = f_1/\varepsilon_f \quad \text{and} \quad C = 1 \tag{44}$$

This model can be written as:

$$\frac{dF}{dt} = \frac{dF}{ds}\frac{ds}{dt} = |v|\frac{dF}{ds} = \frac{f_1}{\varepsilon_f}\left(v - |v|\frac{F}{f_1} \right) \tag{45}$$

The first order model does not give static friction, nor does it give a friction peak at a specific break-away distance. This can, however, be achieved by a second order model with:

$$\begin{aligned} A &= \begin{bmatrix} -1/(\eta\varepsilon_f) & 0 \\ 0 & -1/\varepsilon_f \end{bmatrix}, \\ B &= \begin{bmatrix} f_1/(\eta\varepsilon_f) \\ -f_2/\varepsilon_f \end{bmatrix} \quad \text{and} \quad C = \begin{bmatrix} 1 & 1 \end{bmatrix} \end{aligned} \tag{46}$$

where $f_1 - f_2$ corresponds to kinetic friction reached exponentially as $s \to \infty$.

Models for Lubricated Contacts

In [10] and [14] a model based on the hydrodynamics of a lubricated journal bearing is introduced. The model stresses the dynamics of the friction force. The eccentricity e of the bearing is an important variable in determining the friction force. A simplified model is given by:

$$F = K_1\left(\varepsilon - \varepsilon_{tr}\right)^2 \Delta + \frac{K_2}{\sqrt{1-\varepsilon^2}} v \tag{47}$$

The first term is due to the shearing of the asperity contacts and the second term is due to the viscosity of the lubricant. The function Δ is an indicator function that is one for $\varepsilon > \varepsilon_{tr}$ and zero otherwise.

The LuGre Model

The LuGre model is a dynamic friction model presented in [9]. The model is related to the bristle interpretation of friction as in [7]. Friction is modeled as the average deflection force of elastic springs. When a tangential force is applied the bristles will deflect like springs. If the deflection is sufficiently large the bristles start to slip. The average bristle deflection for a steady state motion is determined by velocity. It is lower at low velocities, which implies that the steady state deflection decreases with increasing velocity. This models the phenomenon that the surfaces are pushed apart by the lubricant, and models the Stribeck effect. The model has the form:

$$\begin{aligned} \frac{dz}{dt} &= v - \sigma_0 \frac{|v|}{g(v)} z, \\ F &= \sigma_0 z + \sigma_1(v)\frac{dz}{dt} + f(v) \end{aligned} \tag{48}$$

where z denotes the average bristle deflection, σ_0 is the stiffness of the bristles, and $\sigma_1(v)$ the damping, the function $g(v)$ models the Stribeck effect, and $f(v)$ is the viscous friction.

Other models may take into account the influence of temperature on the coefficients of friction, especially related to the contact between non-metallic materials [11][12] or the influence of surface heat treatment [13] or even the influence of chemical composition [15].

5. Friction influence on inverted pendulum control - results and discussions

In order to analyze dry friction of the bearing on the inverted pendulum control law it has assumed a set of friction characteristic described by three and four parameters. It has indicated with $\mu(\dot{x})$ and $f(\dot{\theta})$ friction force characteristic and friction torque characteristic respectively.

The influence has been studied for two cases:

Case 1: dry friction in slide bearing and no friction in the joint bearing;
Case 2: no friction in slide bearing and friction in the joint bearing.

5.1. Case 1

The friction force is given by the following equation:

$$F_{fric} = -\mu(\dot{x})N \tag{49}$$

with:

$$N = (m_p + m_c)g + lm_p\left(\cos(\theta)\dot{\theta}^2 + \sin(\theta)\ddot{\theta}\right) \tag{50}$$

The friction characteristic is indicated in figure 4. It is a non linear function described by relation (51).

$$\mu(\dot{x}) = \frac{a\dot{x}}{b^2 + \dot{x}^2} + c\dot{x}^2 \tag{51}$$

This function describes the well known Stribeck curve. It is possible setting up the parameter a, b, c in order to fit the curve to real data. In the figure 4 and 5 is plotted the response of the system.

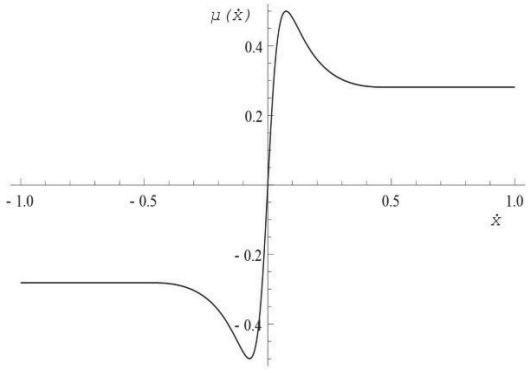

Fig. 4. Non-linear friction characteristic

In figure 5 is indicated the pendulum displacement vs. time and one can see that the response is characterized by an oscillating behavior near to equilibrium position.

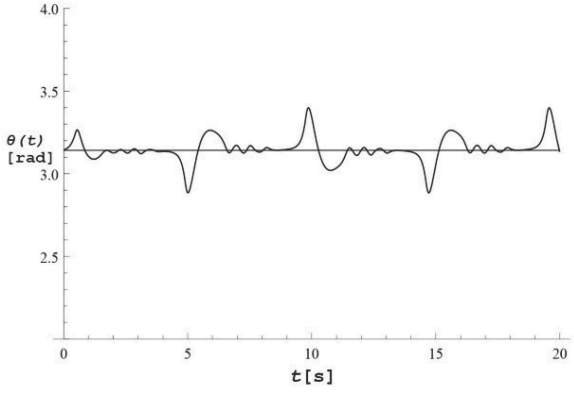

Fig. 5. Pendulum displacement vs. time for continuum non-linear friction model

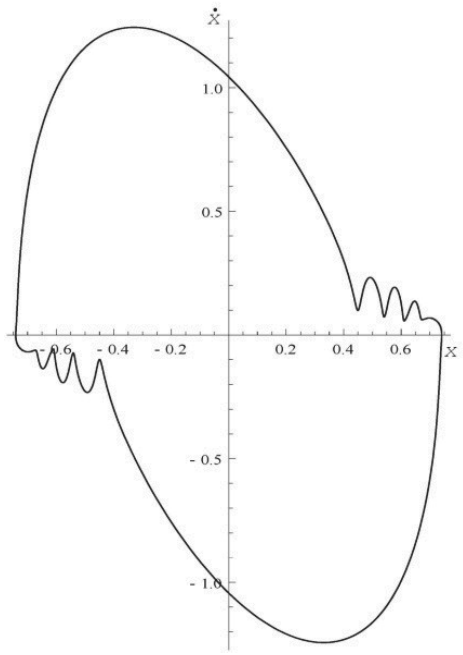

Fig. 6. Cart velocity vs. cart displacement for continuum non-linear friction model

In figure 6 is shown the cart velocity vs. cart displacement. By the picture is evident the periodicity of the response since the phase trajectory is a closed curve. Furthermore, in figure 6 one can see the effects of the smooth transition from static to kinetic friction on the system response.

In the figures 8 and 9, 11 and 12 and 14 and 15 is indicated dynamical behavior of the cart pendulum system in friction conditions described by the models of figures 7, 10 and 13. One can see that for friction model with abrupt transition from static to kinetic friction the disappearing of high order harmonic response.

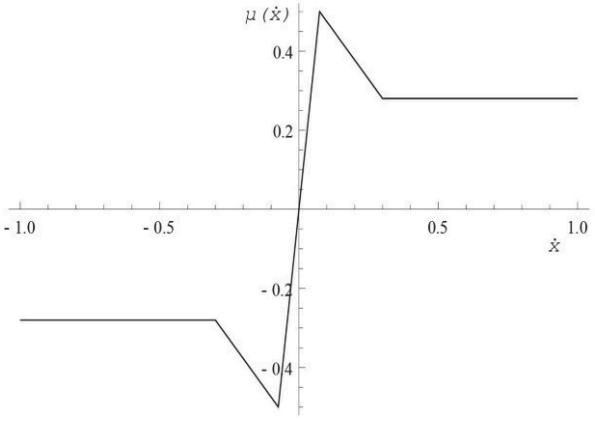

Fig. 7. Piecewise friction linear characteristic - case 1a

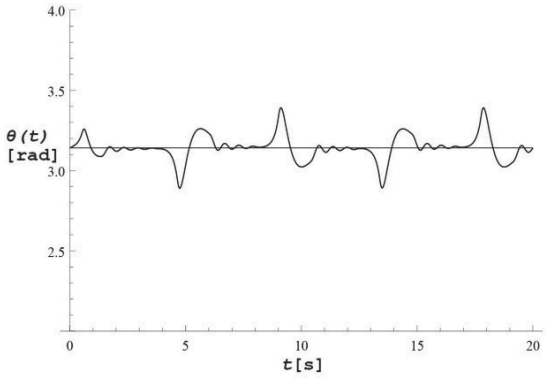

Fig. 8. Pendulum displacement vs. time for piecewise linear friction model - case 1a

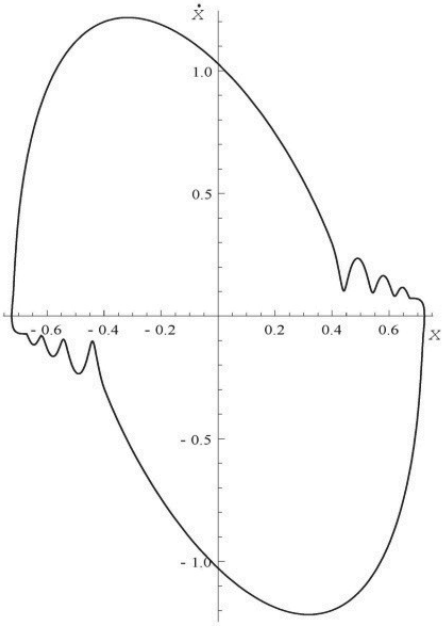

Fig. 9. Cart velocity vs. cart displacement for piecewise linear friction model - case 1a

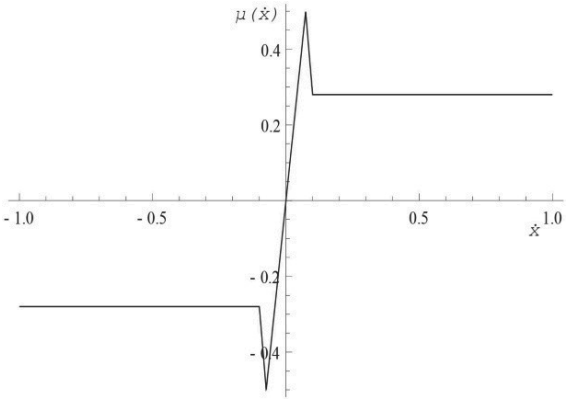

Fig. 10. Piecewise friction linear characteristic - case 1b

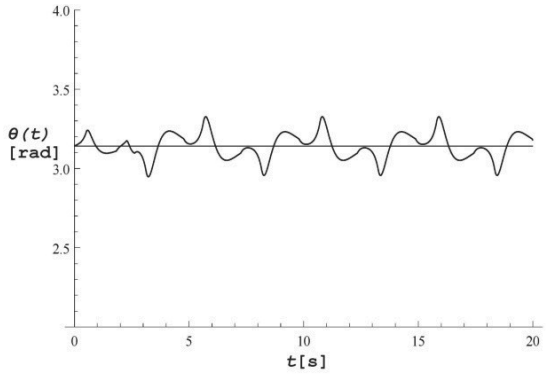

Fig. 11. Pendulum displacement vs. time for piecewise linear friction model - case 1b.

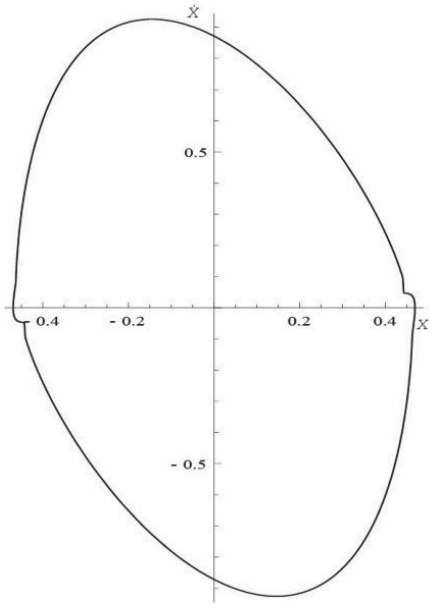

Fig. 12. Cart velocity vs. cart displacement for piecewise linear friction model - case 1b

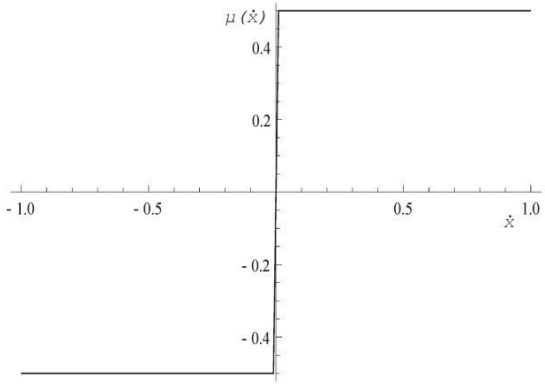

Fig. 13. Piecewise friction linear characteristic -case 1c

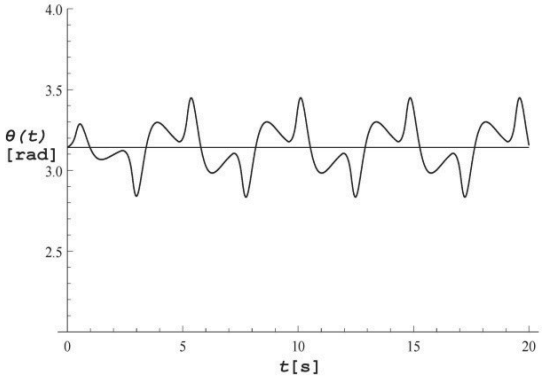

Fig. 14. Pendulum displacement vs. time for piecewise linear friction model – case 1c

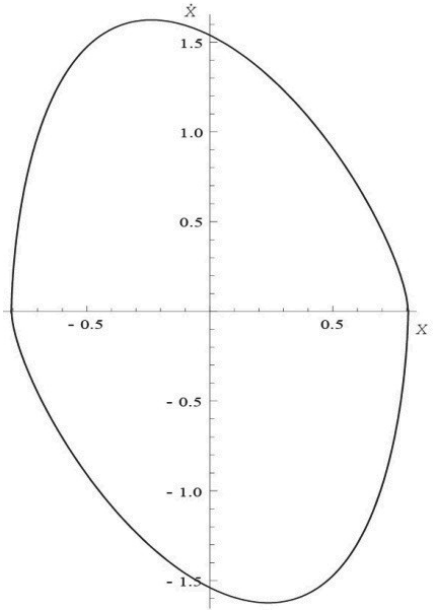

Fig. 15. Cart velocity vs. cart displacement for piecewise linear friction model - case 1c

For a friction piecewise linear function described by three parameters and indicated in figure 16 a simulation has been carried out for evaluating the response of cart pendulum vs. friction parameters. The parameters are named:

μ_S = static coefficient

μ_C = kinetic coefficient

v_C = velocity parameter

Putting this friction model characteristic in the equation (49) and substituting in equation (1), a non-linear system is obtained. This system is difficult to integrate for the presence of the friction force discontinuity. In order to overcome this issue it has been used a numerical methods based on the results of researches indicated in [17].

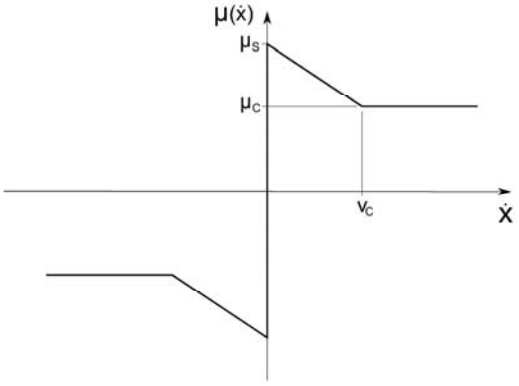

Fig. 16. Piecewise friction characteristic model

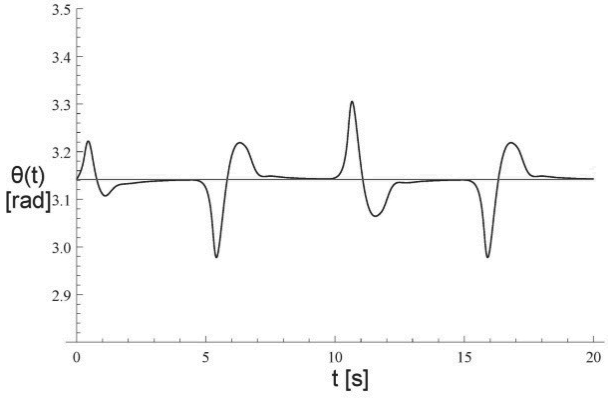

Fig. 17. Pendulum displacement vs. time for $\mu_S = 0.3$ and $\mu_C = 0.2$

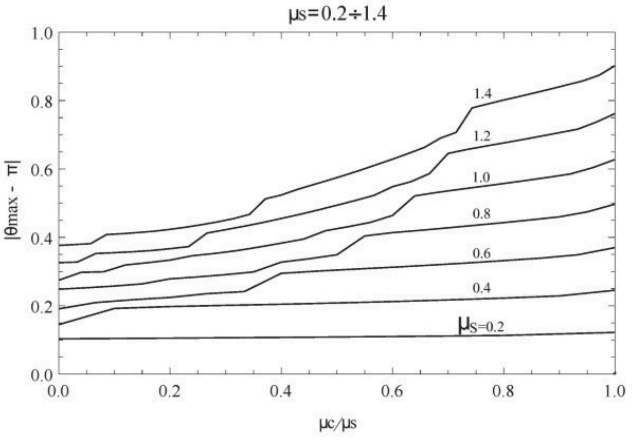

Fig. 18. Pendulum displacement offset vs. kinetic-static friction ratio

In figure 17 it is shown the response of the system for $\mu_S = 0.3$ and $\mu_C = 0.2$, following a small perturbation of upright position.

By repeating this simulation, for different values of μ_C and μ_S , we obtained the plot of figure 18. In this figure it is shown the pendulum offset than upright position vs. kinetic and static friction parameter ratio for different values of the static friction parameter.

By this figure one can see that, the offset of the pendulum displacement become higher to increasing of μ_C and μ_S ratio, with a slope that increases with the increase of μ_S .

5.2. Case 2

Before analyzing the dry friction in the joint on the inverted pendulum control it has assumed a viscous friction model. The friction torque is given by the following equation:

$$C_{fric} = \sigma \dot{\theta} \tag{52}$$

where σ is the *viscous coefficient*.

In the figure 19-24 are shown the system responses, in the $\dot{\theta} - \theta$ and $\theta - t$ plane, for different values of σ. By comparing results with that indicated in figures 2 and 3 is evident that the viscous friction leads to a deterioration of system stability. If viscous friction grows beyond a certain threshold value, dependent of the control law, the system becomes unstable. So as indicated in figure 23 and 24.

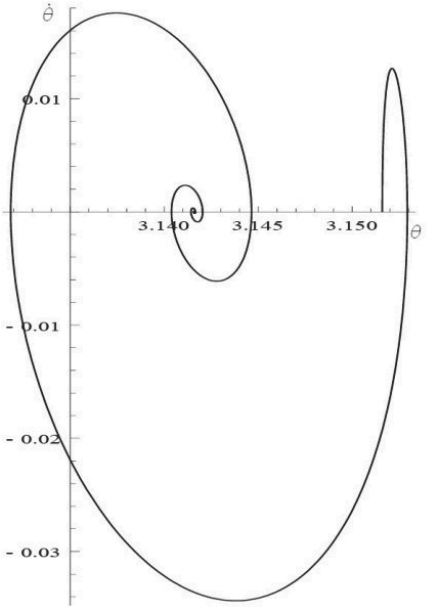

Fig. 19. Angular velocity vs. angular rotation of pendulum for viscous friction –σ=0.01

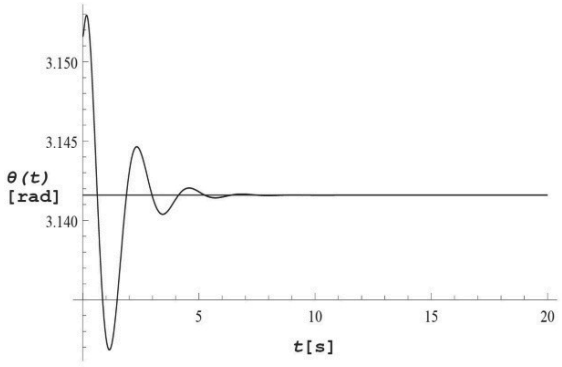

Fig. 20. Pendulum displacement vs. Time for viscous friction - σ=0.01

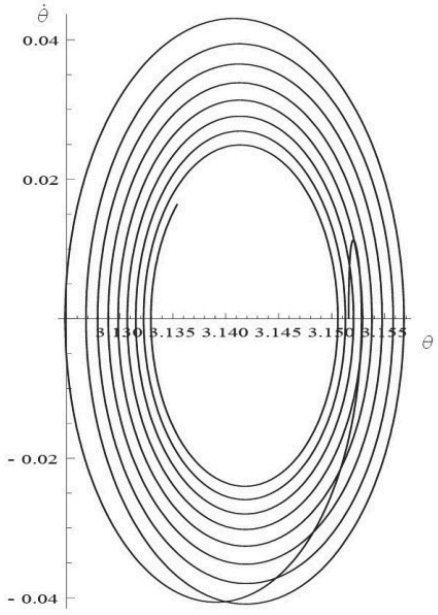

Fig. 21. Angular velocity vs. angular rotation of pendulum for viscous friction – σ=0.02

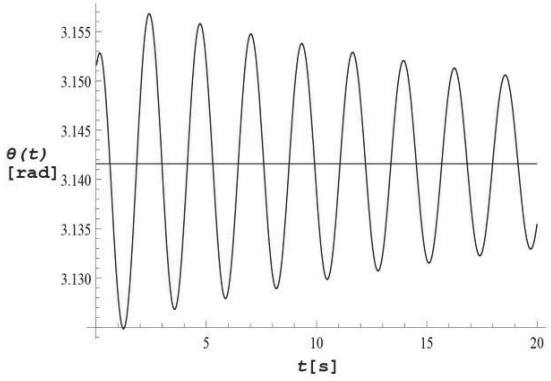

Fig. 22. Pendulum displacement vs. Time for viscous friction - σ=0.02

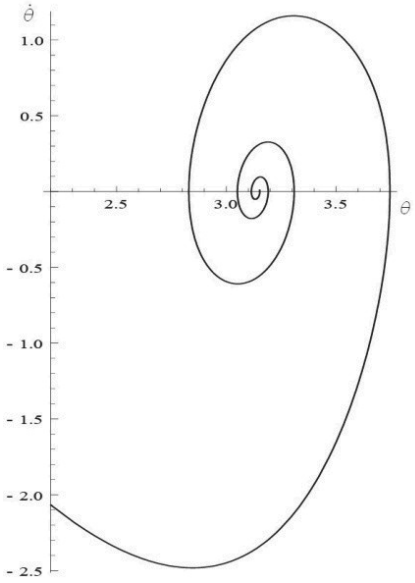

Fig. 23. Angular velocity vs. angular rotation of pendulum for viscous friction – σ=0.03

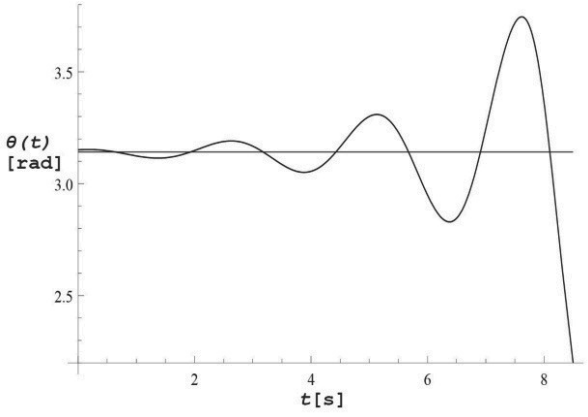

Fig. 24. Pendulum displacement vs. Time for viscous friction - σ=0.03

If the stabilization control law is designed applying the LQ method to the model with viscous friction, system response (Fig. 25 and 26) is like the system with no friction.

Returning to the case of dry friction model, the friction torque is given by the following equation:

$$C_{fric} = -f(\dot{\theta})\frac{d}{2}N_p \tag{53}$$

with:

$$N_p = m_p g + l m_p\left(\cos(\theta)\dot{\theta}^2 + \sin(\theta)\ddot{\theta}\right) \tag{54}$$

In (53) d is the diameter of the journal and it is assumed to be 0.03m.

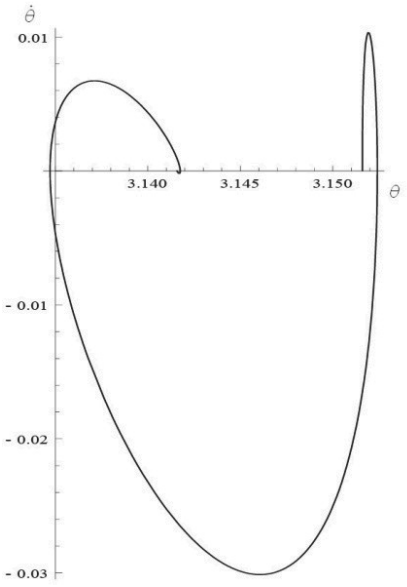

Fig. 25. Angular velocity vs. angular rotation of pendulum for viscous friction taken into account in the LQ Regulator – σ=0.03

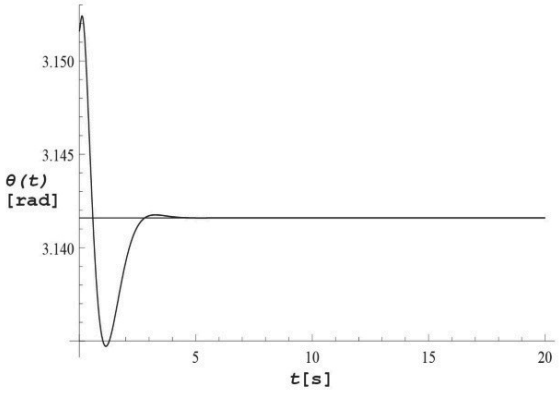

Fig. 26. Pendulum displacement vs. Time for viscous friction taken into account in the LQ Regulator – σ=0.03

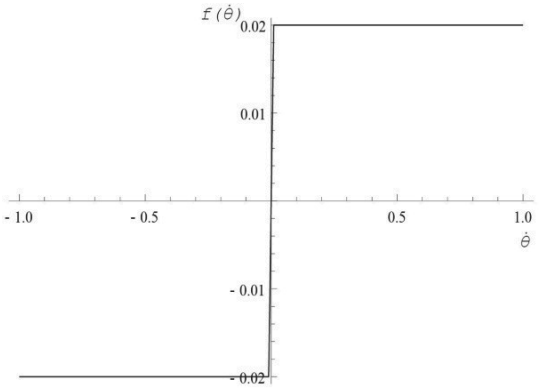

Fig. 27. Piecewise friction linear characteristic -case 2a

In the figures 28 and 29, 31 and 32, 34 and 35, 37 and 38 is shown dynamical behavior of the cart pendulum system in friction conditions described by the models of figures 27, 30, 33 and 36. One can see that, for small values of friction, the system is asymptotically stable (Fig. 28-29) and for higher friction values shows periodic responses (Fig. 31-32 and Fig. 34-35)or becomes unstable (Fig 37-38).

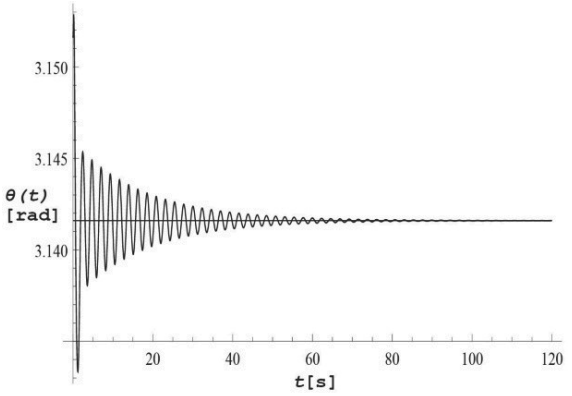

Fig. 28. Pendulum displacement vs. time for piecewise linear friction model – case 2a

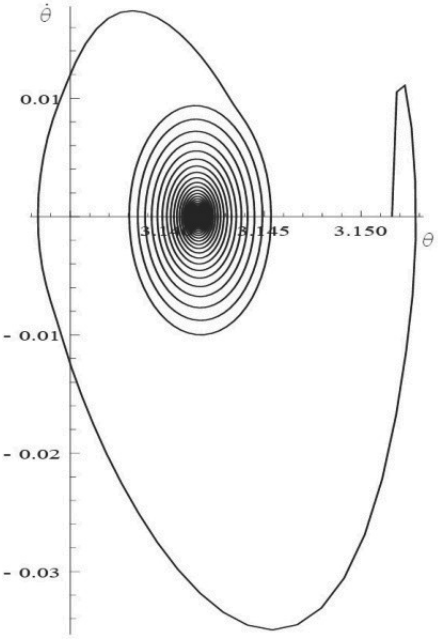

Fig. 29. Angular velocity vs. angular rotation of pendulum for piecewise linear friction model – case 2a

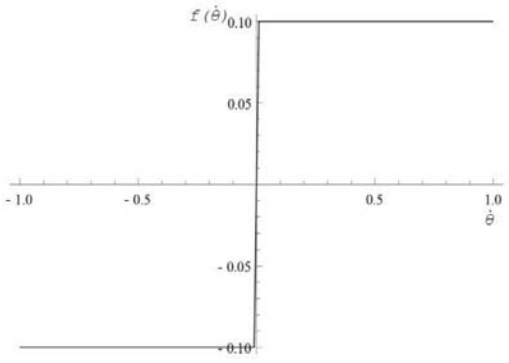

Fig. 30. Piecewise friction linear characteristic -case 2b

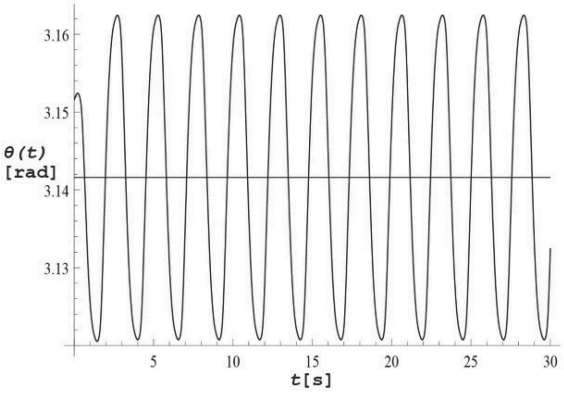

Fig. 31. Pendulum displacement vs. time for piecewise linear friction model – case 2b

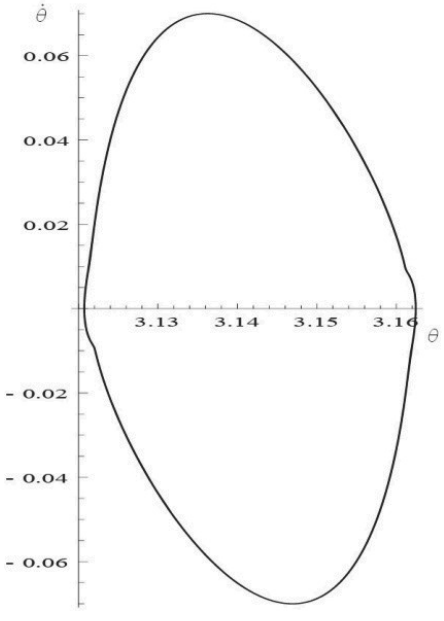

Fig. 32. Angular velocity vs. angular rotation of pendulum for piecewise linear friction model – case 2b

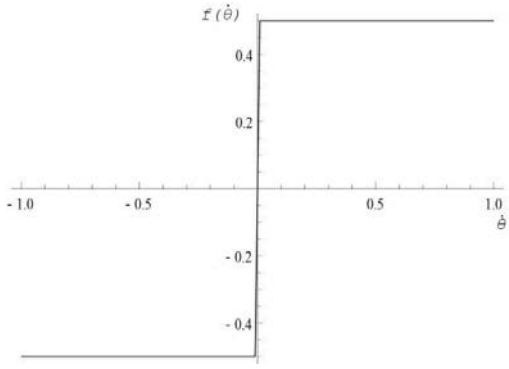

Fig. 33. Piecewise friction linear characteristic -case 2c

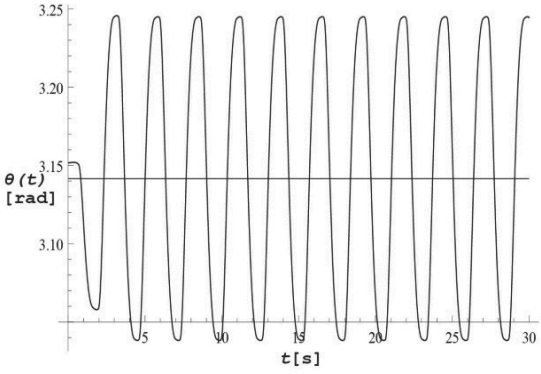

Fig. 34. Pendulum displacement vs. time for piecewise linear friction model – case 2c

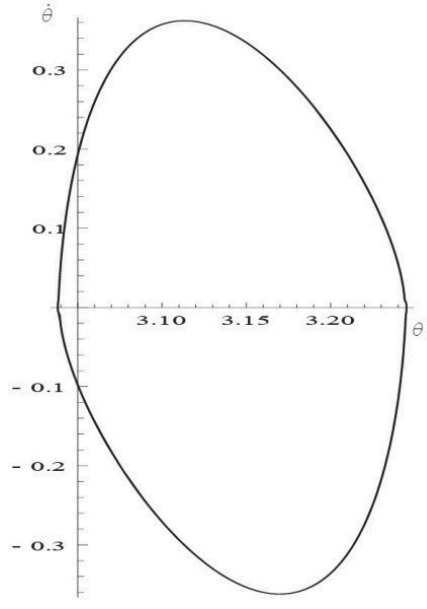

Fig. 35. Angular velocity vs. angular rotation of pendulum for piecewise linear friction model – case 2c

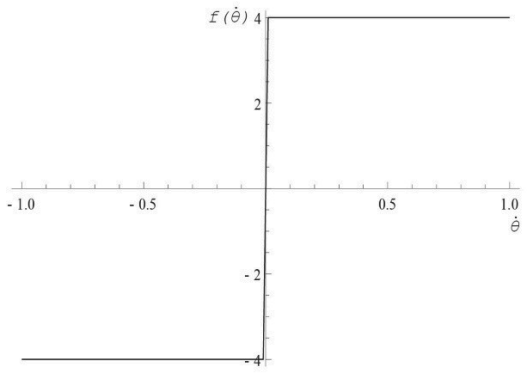

Fig. 36. Piecewise friction linear characteristic -case 2d

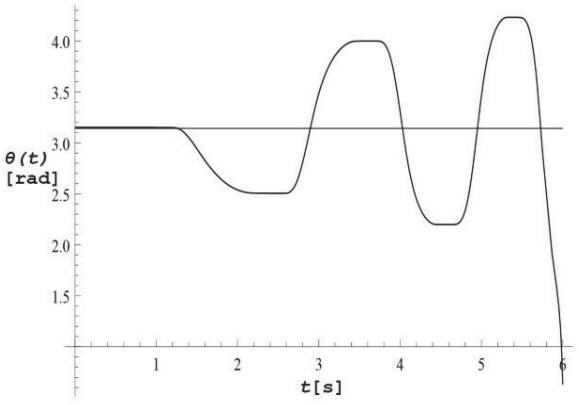

Fig. 37. Pendulum displacement vs. time for piecewise linear friction model – case 2d

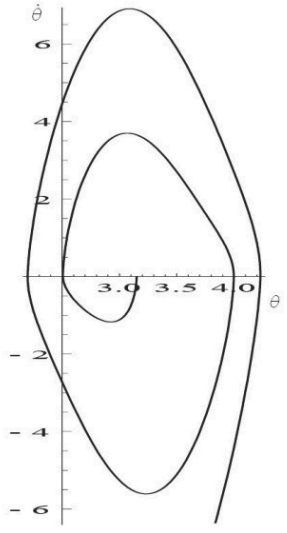

Fig. 38. Angular velocity vs. angular rotation of pendulum for piecewise linear friction model – case 2d

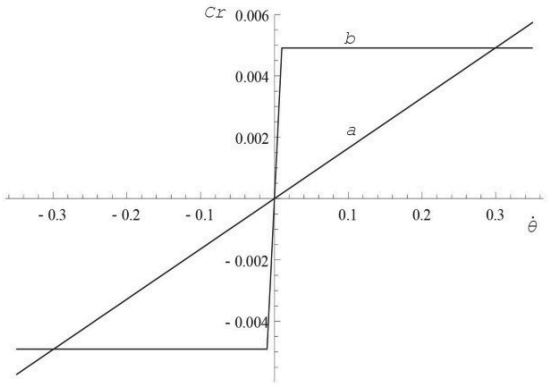

Fig. 39. Comparison between the friction torque in the pivot b) (friction model: case 3) and the corresponding viscous model used for the LQ Regulator a) - case 2e

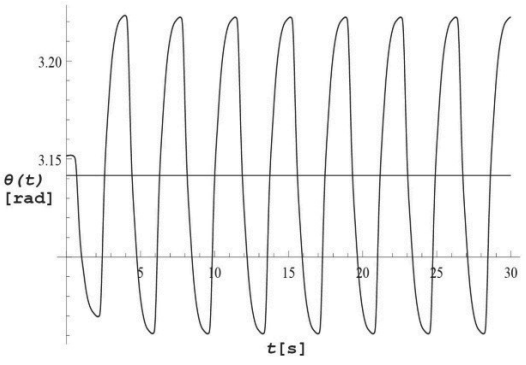

Fig. 40. Pendulum displacement vs. time for piecewise linear friction model – case 2e

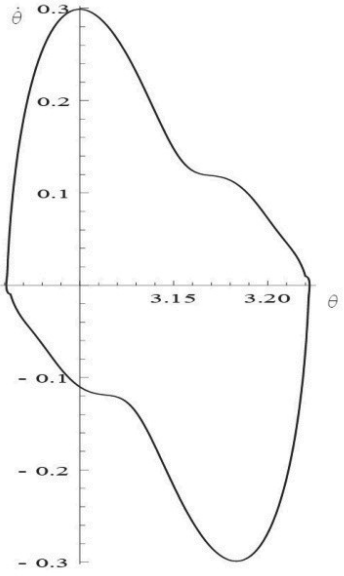

Fig. 41. Angular velocity vs. angular rotation of pendulum for piecewise linear friction model – case 2e

In Figures 40-41 and 43-44 it is shown the system response, for friction of figure 33 and 36, for a controller designed by applying the LQ method to the model with viscous friction.

Viscous coefficient was chosen by equating the resistant torques, given by the two friction models (dry and viscous), at the maximum angular velocities expected. In figures 39 and 42 one can see the comparison between the friction characteristic. In this figures was assumed $N_{p=} m_p g$.

As one can see, such a control law improves the response of the system in to dry friction condition. This is more evident in the case of the friction model of figure 36, in which the system turns from unstable into stable system.

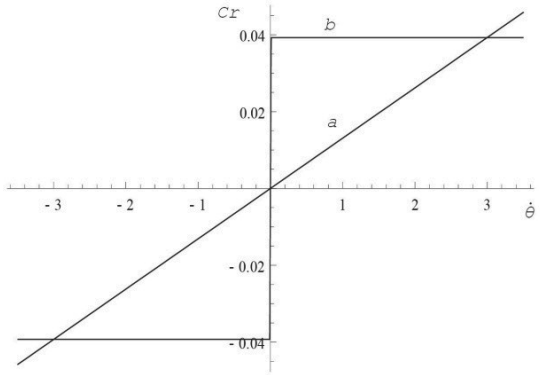

Fig. 42. Comparison between the friction torque in the pivot b) (friction model: case 2d) and the corresponding viscous model used for the LQ Regulator a) - case 2f

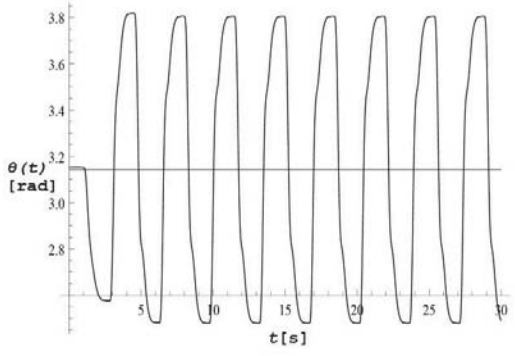

Fig. 43. Pendulum displacement vs. time for piecewise linear friction model – case 2f

In this paper has been proposed an analysis for investigation of the dry friction of bearing influence on dynamics and control of the inverted pendulum system. The assumed friction models have allowed us to highlight the influence of static and dynamic coefficients on the control. Results are proposed in a picture that allows to foresee the friction influence on the inverted pendulum dynamics in quick way.

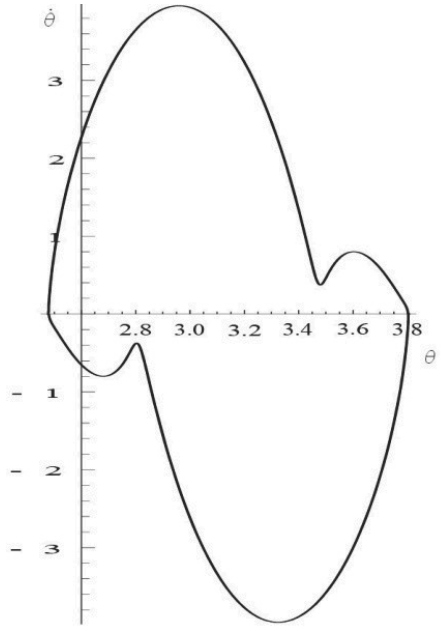

Fig. 44. Angular velocity vs. angular rotation of pendulum for piecewise linear friction model – case 2f

References

[1] H. Olsson, K.J. Åström, C. Canudas de Wit, M. Gfvert, P. Lischinsky, Friction models and friction compensation, European Journal of Control 4/3 (1998) 176-195.

[2] A.J. Morin, New friction experiments carried out at Metz in 1831–1833, Proceedings of the French Royal Academy of Sciences, volume 4, 1833, 1-128.

[3] R. Stribeck, Die wesentlichen Eigenschaften der Gleit- und Rollenlager – The key qualities of sliding and roller bearings, Zeitschrift des Vereines Seutscher Ingenieure, 46(38,39):1342–48,1432–37, 1902.

[4] B. Armstrong-Hélouvry, Control of Machines with Friction, Kluwer Academic Publishers, Boston, Ma., 1991.

[5] D. Karnopp, Computer simulation of slip-stick friction in mechanical dynamic systems, Journal of Dynamic Systems, Measurement, and Control 107/1 (1985) 100-103.

[6] W. Ramberg, W. R. Osgood, Description of stress-strain curves by three parameters, Tech. Note 902, National Advisory Committee for Aeronautics, Washington, 1943.

[7] D.A. Haessig, B. Friedland, On the modelling and simulation of friction, J Dyn Syst Meas Control Trans ASME 113/3 (1991) 354-362.

[8] P.-A. Bliman, M. Sorine, Friction modelling by hysteresis operators. application to Dahl, sticktion and Stribeck effects, Proceedings of the Conference “Models of Hysteresis”, Trento, Italy, 1991.

[9] C. Canudas de Wit, H. Olsson, K. J. Åström, P. Lischinsky, A new model for control of systems with friction 40/3 (1995) 21-26.

[10] A. Harnoy and B. Friedland, Dynamic friction model of lubricated surfaces for precise motion control, In Preprint No. 93-TC-1D-2. Society of Tribologists and Lubrication Engineers, 1993.
[11] G. Wróbel, M. Szymiczek, Influence of temperature on friction coefficient of low density polyethylene, Journal of Achievements in Materials and Manufacturing Engineering 28/1 (2008) 31-34.
[12] J. Myalski, J. Śleziona, Characteristic of polymer sliding materials using to work at elevated temperature, Archives of Materials Science and Engineering 31/2 (2008) 91-94
[13] M. Bonek, L.A. Dobrzański, Functional properties of laser modified surface of tool steel, Journal of Achievements in Materials and Manufacturing Engineering 17 (2006) 313-316.
[14] S. Sharma, D. Hargreaves, W. Scott, Journal bearing performance and metrology issues, Journal of Achievements in Materials and Manufacturing Engineering 32/2 (2009) 98-103.
[15] P. Figiel, S. Zimowski, P. Klimczyk, T. Dziwisz, L. Jaworska, Mechanical and tribological properties of TiC–based composites for ED machining, of Archives of Materials Science and Engineering 33/2 (2008) 83-88.
[16] D. Guida, L. Durso. Dry Friction Influence on the Stability of a Mechanical System with Two Degree of Freedom, Proceedings of the 7th WSEAS International Conference on Non-Linear Analysis, Non-Linear Systems and Chaos, Sofia, 2005, 56-60.
[17] D. Guida, F. Nilvetti, C.M. Pappalardo, Friction induced vibrations of a two degrees of freedom system, (in print).
[18] D. Guida, C.M. Pappalardo. Journal Bearing Parameter Identification. Proceedings of the 11th WSEAS International Conference on Automatic Control, Modellig and Simulation, Istambul, 2009, 475-478.